Stress intensity factor for multiple cracks in an infinite plate using hypersingular integral equations

Razieh Ghorbanpoor
Department of Applied Mathematics,
Ferdowsi University of Mashhad, Mashhad, Iran.
E-mail: ra_ghor@yahoo.com

Jafar Saberi-Nadjafi∗
Department of Applied Mathematics,
Ferdowsi University of Mashhad, Mashhad, Iran.
E-mail: najafi141@gmail.com

Nik Mohd Asri Nik Long
Department of Mathematics, Universiti Putra Malaysia,
43400 Serdang, Selangor, Malaysia.
E-mail: nmasri@upm.edu.my

Majid Erfanian
Department of Science, School of Mathematical Sciences,
University of Zabol, Zabol, Iran.
E-mail: erfaniyan@uoz.ac.ir

Abstract In this paper, numerical solutions of multiple cracks problems in an infinite plate are studied. Hypersingular integral equations (hieq) for the cracks are formulated using the complex potential method. For all kernels such as regular or hypersingular kernels, we are using the appropriate quadrature formulas to solve and evaluate the unknown functions numerically . Furthermore, by using this equation the stress intensity factor (SIF) was calculated for crack tips. For two serial cracks (horizontal) and two dissimilar cracks (horizontal and inclined), our numerical results agree with the previous works.

1. INTRODUCTION

Most of the crack problems are modeled into integral equation of the form

$$\int_\gamma k(\tau, \tau_0) f(\tau) d\tau = p(\tau_0), \qquad (\tau_0 \in \gamma).$$

In this equation, $k(\tau, \tau_0)$ is the kernel of the integral, γ is the crack with linear or curve configuration, the function $f(\tau)$ is unknown, and $p(\tau_0)$ is known. The construction of the kernel $k(\tau, \tau_0)$ is determined by the choice of $f(\tau)$ and $p(\tau_0)$; for example, if $p(\tau_0)$

∗ Corresponding author.

is the resultant force and $f(\tau)$ is the dislocation, then the kernel is weakly singular (see [1, 8, 11, 24]).

The other case is, if $p(\tau_0)$ is the traction and $f(\tau)$ is the dislocation, then $k(\tau, \tau_0)$ is the Cauchy singular (see [12, 21, 22]), in the third case, if $p(\tau_0)$ is the resultant force and $f(\tau)$ is the crack opening displacement (COD), so the kernel $k(\tau, \tau_0)$ will be the Cauchy singular (see [5, 20]), and the last case, if $p(\tau_0)$ are the traction and $f(\tau)$ is the crack opening displacement, then the $k(\tau, \tau_0)$ is a kernel of hypersingular integral (see [14, 15, 18]). The hypersingular is evaluated by collocating the base points within the interval $(-a, a)$. The particular advantage of this approach is that COD can be obtained from the solution of the equation directly. Hadamard was the pioneer researcher that formulated the hypersingular integral equation (hieq) for solving the crack problem (see [13]). The hypothesis in Hadamard formulation is based on the superposition technique and the quadratic polynomial. By a same technique, Chen (see [2, 3]) formulated multiple cracks problems by CODs function and traction on the cracks. It is well known that the crack geometry has a direct effect on stress intensity factors (SIFs). Chen (see [4, 6]) suggested a system of hieq for solving curved crack problem. Nik Long and Eshkuvatov (see [19]) formulated the multiple curved cracks problem in terms of hieq. In this work, the systems of hieq for solving multiple cracks problems with different position of cracks are formulated and solved numerically. For numerical purpose, several examples of multiple cracks problems are considered.

2. Analysis of solving the multiple cracks problem

In this section, we first explain the fundamental of complex variable function method. For this purpose, we introduce

$$\Phi = \varphi' \quad and \quad \Psi = \psi',$$

then, the stress $(\delta_x, \delta_y, \delta_{xy})$, the resultant force (X, Y), and the displacements (u, v) can be shown by the two complex potentials $\varphi(z)$ and $\psi(z)$ as follows [16]:

$$\delta_x + \delta_y = 4Re\Phi(z), \tag{2.1}$$

$$\delta_y - \delta_x + 2i\delta_{xy} = 2[\bar{z}\Phi(z) + \Psi(z)], \tag{2.2}$$

$$f = -Y + iX = \varphi(z) + z\overline{\Phi(z)} + \overline{\psi(z)} + c, \tag{2.3}$$

$$2\eta(u + iv) = \kappa\varphi(z) - z\overline{\Phi(z)} - \overline{\psi(z)}, \tag{2.4}$$

where η is the shear modulus for plane elasticity, $\kappa = \dfrac{3 - \upsilon}{1 + \upsilon}$ and $\kappa = 3 - 4\upsilon$ are used for plane strain and plane stresse, respectively, υ is placed as Poisson's ratio, z is a complex variable, and a bar that is placed over the function represents for the conjugated value. The derivative in a specified and defined direction for Eq. (2.3) is presented by

$$J(z, \bar{z}, \frac{d\bar{z}}{dz}) = \frac{d}{dz}\{-Y + iX\} = \Phi(z) + \overline{\Phi(z)} + \frac{d\bar{z}}{dz}(z\overline{\Phi'(z)} + \overline{\Psi(z)}) = N + iT, \tag{2.5}$$

where J represents the normal tractions and tangential tractions through the part $\overline{z, z + dz}$. It is note that the value of J not only depends on the location of point z,

but also on the orientation of the segment $\dfrac{d\bar{z}}{dz}$.

The complex potential for plane elasticity will be evaluated by substituting two point dislocations with known intensity $H(-H)$ at the point $z = s$ and $(z = s + ds)$, respectively, we have

$$\varphi(z) = -H\frac{ds}{z-s}, \qquad \psi(z) = -\overline{H}\frac{ds}{s-z} - H\frac{d\bar{s}}{s-z} + H\frac{\bar{s}ds}{(s-z)^2}. \tag{2.6}$$

Substituting H and $-H$ by $-\dfrac{\xi(s)}{2\pi}$ and $-\dfrac{\overline{\xi(s)}}{2\pi}$, respectively, in Eq. (2.6) and applying the integration on the right side of $\varphi(z)$ and $\psi(z)$, give

$$\varphi(z) = \frac{1}{2\pi}\int_\gamma \frac{\xi(s)ds}{s-z},$$

$$\psi(z) = \frac{1}{2\pi}\int_\gamma \frac{\xi(s)d\bar{s}}{s-z} + \frac{1}{2\pi}\int_\gamma \frac{\overline{\xi(s)}ds}{s-z} - \frac{1}{2\pi}\int_\gamma \frac{\bar{s}\xi(s)ds}{(s-z)^2}, \tag{2.7}$$

where γ state the crack construction. Making substitution Eq. (2.7) into Eq. (2.4) and letting z tends s_0^+ (s_0^-) the upper (lower) side of crack faces, respectively, then using the generalized Plemelj formula and revising s_0 as s, results (see [4])

$$2\eta(u(s) + iv(s))_j = i(k+1)\xi(s) \qquad (s \in \gamma) \tag{2.8}$$

when

$$(u(s) + iv(s))_j = (u(s) + iv(s))^+ - (u(s) + iv(s))^-$$

represents the crack opening displacement (COD) of the crack, which has the following attributes

$$\xi(s) = O[(s - s_A)^{1/2}], \quad \xi(s) = O[(s - s_B)^{1/2}] \tag{2.9}$$

at the neighborhood of the left crack tip A and the right crack tip B (see Fig.1(a,b)). First, we assume hieq in the case of Hamadard finite part integral as

$$\frac{1}{\pi}\fint_\gamma \frac{\xi(s)ds}{(s-s_0)^2}.$$

Thus, in [7] the hieq for a single inclined crack in infinite plate is formulated by putting two points dislocation at $z = s$ and $z = s + ds$ as

$$\frac{1}{\pi}\fint_\gamma \frac{\xi(s)ds}{(s-s_0)^2} + \frac{1}{\pi}\int_\gamma M(s,s_0)\xi(s)ds + \frac{1}{\pi}\int_\gamma L(s,s_0)\overline{\xi(s)}ds$$
$$= N(s_0) + iT(s_0), \tag{2.10}$$

in which $M(s, s_0)$ and $L(s, s_0)$ are stated as

$$M(s, s_0) = \frac{1}{2}\left[\exp{(2i\alpha)}\frac{-1}{(Q - Q_0)^2} + \exp{(-2i\alpha_0)}\frac{1}{\left(\overline{Q} - \overline{Q_0}\right)^2}\right],$$

$$L(s, s_0) = \frac{1}{2} \left[(\exp(-2i\alpha) + \exp(-2i\alpha_0)) \frac{1}{(\overline{Q} - \overline{Q_0})^2} \right]$$
$$- \frac{1}{2} \left[\exp(-2i(\alpha + \alpha_0)) \frac{2(Q - Q_0)}{(\overline{Q} - \overline{Q_0})^3} \right],$$

$$Q = z_{k0} + t \exp(i\alpha), \quad Q_0 = z_{k0} + t_0 \exp(i\alpha_0).$$

in which $\xi(s)$ is dislocation distribution through the inclined crack. The first integral, in Eq. (2.10), with equal sign on, states the hypersingular integral and it is explained in the sense of the Hamadard finite part integral.
Now we discuss the traction influences between two cracks (similar or dissimilar)(see Fig.1(c)). In crack-1 (crack AB)(see Fig.1(c)) if the dislocation distribution is a $\xi_1(s_1)$,
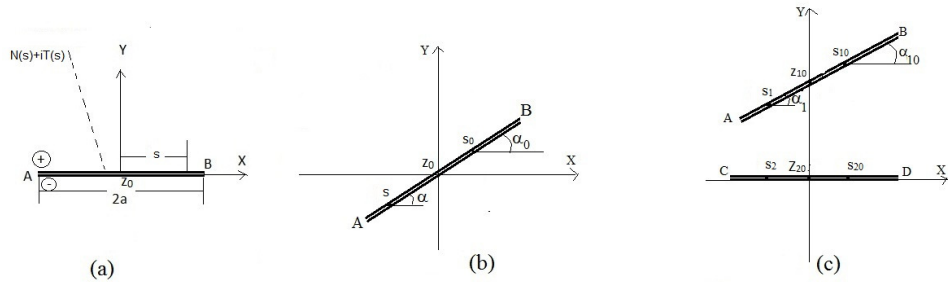
FIGURE 1. (a) A straight crack ($\alpha = 0$), (b) An inclined crack with angles α, (c) Two dissimilar cracks with angles α_1 and $\alpha_2 = 0$, respectively.

points $z = s_{10}$ and $dz = ds_{10}$ are points dislocation and there is the traction influences between the two cracks (similar or dissimilar), then the hieq of crack-1 is

$$\frac{1}{\pi} \oint_{\gamma_1} \frac{\xi_1(s_1) ds_1}{(s_1 - s_{10})^2} + \frac{1}{\pi} \int_{\gamma_1} M(s_1, s_{10}) \xi_1(s_1) ds_1 + \frac{1}{\pi} \int_{\gamma_1} L(s_1, s_{10}) \overline{\xi_1(s_1)} ds_1$$
$$= N_{11}(s_{10}) + i T_{11}(s_{10}), \quad (2.11)$$

where

$$M(s_1, s_{10}) = \frac{1}{2} \left[\exp(2i\alpha_1) \frac{-1}{(Q_1 - Q_{10})^2} + \exp(-2i\alpha_{10}) \frac{1}{(\overline{Q_1} - \overline{Q_{10}})^2} \right],$$

$$L(s_1, s_{10}) = \frac{1}{2} \left[(\exp(-2i\alpha_1) + \exp(-2i\alpha_{10})) \frac{1}{\left(\overline{Q_1} - \overline{Q_{10}}\right)^2} \right]$$
$$- \frac{1}{2} \left[\exp(-2i(\alpha_1 + \alpha_{10})) \frac{2(Q_1 - Q_{10})}{\left(\overline{Q_1} - \overline{Q_{10}}\right)^3} \right].$$

$$Q_1 = z_{10} + t_1 \exp(i\alpha_1), \quad Q_{10} = z_{10} + t_{10} \exp(i\alpha_{10}).$$

where α_1 and α_{10} are inclined angles at points s_1 and s_{10}, respectively. The affection from the dislocation distribution on crack-2 can be expressed as

$$\frac{1}{\pi} \int_{\gamma_2} \frac{\xi_2(s_2) ds_2}{(s_2 - s_{10})^2} + \frac{1}{\pi} \int_{\gamma_2} M(s_2, s_{10}) \xi_2(s_2) ds_2 + \frac{1}{\pi} \int_{\gamma_2} L(s_2, s_{10}) \overline{\xi_2(s_2)} ds_2$$
$$= N_{21}(s_{10}) + iT_{21}(s_{10}), \quad (2.12)$$

where

$$M(s_2, s_{10}) = \frac{1}{2} \left[\exp(2i\alpha_2) \frac{-1}{(Q_2 - Q_{10})^2} + \exp(-2i\alpha_{10}) \frac{1}{\left(\overline{Q_2} - \overline{Q_{10}}\right)^2} \right],$$

$$L(s_2, s_{10}) = \frac{1}{2} \left[(\exp(-2i\alpha_2) + \exp(-2i\alpha_{10})) \frac{1}{\left(\overline{Q_2} - \overline{Q_{10}}\right)^2} \right]$$
$$- \frac{1}{2} \left[\exp(-2i(\alpha_2 + \alpha_{10})) \frac{2(Q_2 - Q_{10})}{\left(\overline{Q_2} - \overline{Q_{10}}\right)^3} \right],$$

$$Q_2 = z_{20} + t_2 \exp(i\alpha_2).$$

Due to the fact that $s_2 - s_{10} \neq 0$, each integral in Eq. (2.12) is regular and $\xi_1(s_1)$ and $\xi_2(s_2)$ satisfy Eq. (2.9). Using the superpositions of $\xi_1(s_1)$ on crack-1 (Eq. (2.11)), and $\xi_2(s_2)$ on crack-2 (Eq. (2.12)), the hieq of crack-1 is expressible as

$$\frac{1}{\pi} \fint_{\gamma_1} \frac{\xi_1(s_1) dt_1}{(s_1 - s_{10})^2} + \frac{1}{\pi} \int_{\gamma_1} M(s_1, s_{10}) \xi_1(s_1) ds_1 + \frac{1}{\pi} \int_{\gamma_1} L(s_1, s_{10}) \overline{\xi_1(s_1)} ds_1$$
$$+ \frac{1}{\pi} \int_{\gamma_2} \frac{\xi_2(s_2) ds_2}{(s_2 - s_{10})^2} + \frac{1}{\pi} \int_{\gamma_2} M(s_2, s_{10}) \xi_2(s_2) ds_2 + \frac{1}{\pi} \int_{\gamma_2} L(s_2, s_{10}) \overline{\xi_2(s_2)} ds_2$$
$$= N_1(s_{10}) + iT_1(s_{10}), \quad (2.13)$$

where

$$N_1(s_{10}) + iT_1(s_{10}) = N_{11}(s_{10}) + iT_{11}(s_{10}) + N_{12}(s_{10}) + iT_{12}(s_{10}), \quad s_{10} \in \gamma_1,$$

is the traction utilized at point s_{10} of crack-1, that can be obtained from the boundary condition. In Eq. (2.13), the first, second, and third integrals indicate the effect on crack-1 applied by the dislocation's distribution in the crack-1 itself, while the fourth, fifth, and sixth integrals demonstrate the effect of dislocation distribution from crack-2 on crack-1. The first integral in Eq. (2.13) is hypersingular, while the rests are

regular. Similarly, for crack-2 we have

$$\frac{1}{\pi}\oint_{\gamma_2}\frac{\xi_2(s_2)ds_2}{(s_2-s_{20})^2}+\frac{1}{\pi}\int_{\gamma_2}M(s_2,s_{20})\xi_2(s_2)ds_2+\frac{1}{\pi}\int_{\gamma_2}L(s_2,s_{20})\overline{\xi_2(s_2)}ds_2$$

$$+\frac{1}{\pi}\int_{\gamma_1}\frac{\xi_1(s_1)ds_1}{(s_1-s_{20})^2}+\frac{1}{\pi}\int_{\gamma_1}M(s_1,s_{20})\xi_1(s_1)ds_1+\frac{1}{\pi}\int_{\gamma_1}L(s_1,s_{20})\overline{\xi_1(s_1)}ds_1$$

$$= N_2(s_{20})+iT_2(s_{20}), \quad (2.14)$$

where

$$N_2(s_{20})+iT_2(s_{20}) = N_{21}(s_{20})+iT_{21}(s_{20})+N_{22}(s_{20})+iT_{22}(s_{20}), \quad s_{20}\in\gamma_2,$$

is the traction utilized at point s_{20} of crack-2, and for $j=1,2$

$$M(s_j,s_{20}) = \frac{1}{2}\left[\exp\left(2i\alpha_j\right)\frac{-1}{\left(Q_j-Q_{20}\right)^2}+\exp\left(-2i\alpha_{20}\right)\frac{1}{\left(\overline{Q_j}-\overline{Q_{20}}\right)^2}\right],$$

$$L(s_j,s_{20}) = \frac{1}{2}\left[\left(\exp\left(-2i\alpha_j\right)+\exp\left(-2i\alpha_{20}\right)\right)\frac{1}{\left(\overline{Q_j}-\overline{Q_{20}}\right)^2}\right]$$

$$-\frac{1}{2}\left[\exp\left(-2i\left(\alpha_j+\alpha_{20}\right)\right)\frac{2\left(Q_j-Q_{20}\right)}{\left(\overline{Q_j}-\overline{Q_{20}}\right)^3}\right],$$

that

$$Q_j = z_{j0}+t_j\exp\left(i\alpha_j\right), \quad Q_{20} = z_{20}+t_{20}\exp\left(i\alpha_{20}\right), \; j=1,2.$$

The first three integrals in Eq. (2.14) display the influence on crack-2 affected by the dislocation's distribution on the crack-2 itself, whereas the fourth, fifth, and sixth integrals denote the influence of dislocation distribution from the crack-1 on crack-2. Eqs. (2.13) and (2.14) could be solved simultaneously for $\xi_1(s_1)$ and $\xi_2(s_2)$.
Obviously, if two cracks are faraway, then $|s_2-s_{10}|$ and $|s_1-s_{20}|$ come close to infinity which caused the forth, fifth, and sixth integrals in Eqs. (2.13) and (2.14) are disappeared. In this case the solution for Eqs. (2.13) and (2.14) is the same as the resolvent for a single crack problem and so a closed-form resolvent is available [9].

3. Length coordinate method

Now, consider a mapping of cracks on a real axis t with the mapping function $s_1(t_1)$ and $s_2(t_2)$ which are defined as

$$\xi_1(s_1)|_{s_1=s_1(t_1)} = \sqrt{(a_1^2-t_1^2)}H_1(t_1), \quad \text{where } H_1(t_1)=H_{11}(t_1)+iH_{12}(t_1), \quad (3.1)$$

$$\xi_2(s_2)|_{s_2=s_2(t_2)} = \sqrt{(a_2^2-t_2^2)}H_2(t_2), \quad \text{where } H_2(t_2)=H_{21}(t_2)+iH_{22}(t_2). \quad (3.2)$$

Using the transformations, Eqs. (3.1) and (3.2), Eqs. (2.13) and (2.14) , respectively, can be expressed as

$$I_1(t_{10}) + I_2(t_{10}) + I_3(t_{10}) + I_4(t_{10}) + I_5(t_{10}) + I_6(t_{10})$$
$$= N_1(t_{10}) + iT_1(t_{10}), \qquad (3.3)$$
$$R_1(t_{20}) + R_2(t_{20}) + R_3(t_{20}) + R_4(t_{20}) + R_5(t_{20}) + R_6(t_{20})$$
$$= N_2(t_{20}) + iT_2(t_{20}), \qquad (3.4)$$

where

$$I_1(t_{10}) = \frac{1}{\pi} \fint_{-a}^{a} \frac{\sqrt{(a_1^2 - t_1^2)}}{(t_1 - t_{10})^2} H_1(t_1) A_1(t_1, t_{10}) dt_1,$$

$$I_2(t_{10}) = \frac{1}{\pi} \int_{-a}^{a} \sqrt{(a_1^2 - t_1^2)} H_1(t_1) B_1(t_1, t_{10}) dt_1,$$

$$I_3(t_{10}) = \frac{1}{\pi} \int_{-a}^{a} \sqrt{(a_1^2 - t_1^2)} \overline{H_1(t_1)} C_1(t_1, t_{10}) dt_1,$$

$$I_4(t_{10}) = \frac{1}{\pi} \int_{-a}^{a} \sqrt{(a_2^2 - t_2^2)} H_2(t_2) D_1(t_2, t_{10}) dt_2,$$

$$I_5(t_{10}) = \frac{1}{\pi} \int_{-a}^{a} \sqrt{(a_2^2 - t_2^2)} H_2(t_2) E_1(t_2, t_{10}) dt_2,$$

$$I_6(t_{10}) = \frac{1}{\pi} \int_{-a}^{a} \sqrt{(a_2^2 - t_2^2)} \overline{H_2(t_2)} F_1(t_2, t_{10}) dt_2,$$

and

$$R_1(t_{20}) = \frac{1}{\pi} \fint_{-a}^{a} \frac{\sqrt{(a_2^2 - t_2^2)}}{(t_2 - t_{20})^2} H_2(t_2) A_2(t_2, t_{20}) dt_2,$$

$$R_2(t_{20}) = \frac{1}{\pi} \int_{-a}^{a} \sqrt{(a_2^2 - t_2^2)} H_2(t_2) B_2(t_2, t_{20}) dt_2,$$

$$R_3(t_{20}) = \frac{1}{\pi} \int_{-a}^{a} \sqrt{(a_2^2 - t_2^2)} \overline{H_2(t_2)} C_2(t_2, t_{20}) dt_2,$$

$$R_4(t_{20}) = \frac{1}{\pi} \int_{-a}^{a} \sqrt{(a_1^2 - t_1^2)} H_1(t_1) D_2(t_1, t_{20}) dt_1,$$

$$R_5(t_{20}) = \frac{1}{\pi} \int_{-a}^{a} \sqrt{(a_1^2 - t_1^2)} H_1(t_1) E_2(t_1, t_{20}) dt_1,$$

$$R_6(t_{20}) = \frac{1}{\pi} \int_{-a}^{a} \sqrt{(a_1^2 - t_1^2)} \overline{H_1(t_1)} F_2(t_1, t_{20}) dt_1,$$

and $A_i, B_i, C_i, D_i, E_i, F_i$ for $i = 1, 2$ are respectively, given by

$$
\begin{aligned}
A_1(t_1, t_{10}) &= \frac{(t_1 - t_{10})^2}{(s_1 - s_{10})^2} \frac{ds_1}{dt_1} \quad, \quad B_1(t_1, t_{10}) = M(s_1, s_{10}) \frac{ds_1}{dt_1}, \\
C_1(t_1, t_{10}) &= L(s_1, s_{10}) \frac{ds_1}{dt_1} \quad, \quad D_1(t_1, t_{10}) = \frac{1}{(s_2 - s_{10})^2} \frac{ds_2}{dt_2}, \\
E_1(t_1, t_{10}) &= M(s_2, s_{10}) \frac{ds_2}{dt_2} \quad, \quad F_1(t_1, t_{10}) = L(s_2, s_{10}) \frac{ds_2}{dt_2},
\end{aligned}
$$

and

$$
\begin{aligned}
A_2(t_2, t_{20}) &= \frac{(t_2 - t_{20})^2}{(s_2 - s_{20})^2} \frac{ds_2}{dt_2} \quad, \quad B_2(t_2, t_{20}) = M(s_2, s_{20}) \frac{ds_2}{dt_2}, \\
C_2(t_2, t_{20}) &= L(s_2, s_{20}) \frac{ds_2}{dt_2} \quad, \quad D_2(t_1, t_{20}) = \frac{1}{(s_1 - s_{20})^2} \frac{ds_1}{dt_1}, \\
E_2(t_1, t_{20}) &= M(s_1, s_{20}) \frac{ds_1}{dt_1} \quad, \quad F_2(t_1, t_{20}) = L(s_1, s_{20}) \frac{ds_1}{dt_1}.
\end{aligned}
$$

4. Solution strategy

The following integration schemes and Gaussian quadrature rule for hypersingular and regular integrals, are used in solving Eqs. (3.3) and (3.4)(see [17, 23]):

$$
\frac{1}{\pi} \fint_{-a}^{a} \frac{\sqrt{a^2 - t^2} \eta(t)}{(t - t_0)^2} dt = \sum_{j=1}^{M+1} W_j(t_0) \eta(t_j) \ (|t_0| < a) \tag{4.1}
$$

and

$$
\frac{1}{\pi} \int_{-a}^{a} \sqrt{a^2 - t^2} \eta(t) dt = \frac{1}{M+2} \sum_{j=1}^{M+1} (a^2 - t_j^2) \eta(t_j),
$$

where $\eta(t)$ is a given function, $M \in \mathbb{Z}$, and

$$
W_j(t_0) = -\frac{2}{M+2} \sum_{n=0}^{M} (n+1) V_j^n U_n \left(\frac{t_0}{a} \right),
$$

in which

$$
V_j^n = \sin \left(\frac{j\pi}{M+2} \right) \sin \left(\frac{(n+1)j\pi}{M+2} \right), \ U_n(s) = \frac{\sin((n+1)\theta)}{\sin \theta}, \ s = cos\theta,
$$

$$
t_0 = t_{0k} = a \cos \left(\frac{k\pi}{M+2} \right), \ t_j = a \cos \left(\frac{j\pi}{M+2} \right), \ j, k = 1, 2, ..., M+1,
$$

$H_1(t_1)$ and $H_2(t_2)$ are defined as follows

$$
\begin{aligned}
H_1(t_1) &= \sum_{n=0}^{M} c_{1n} U_n\left(\frac{t_1}{a_1}\right), \ |t_1| < a_1, \\
H_2(t_2) &= \sum_{n=0}^{M} c_{2n} U_n\left(\frac{t_2}{a_2}\right), \ |t_2| < a_2,
\end{aligned}
\tag{4.2}
$$

where

$$
c_{1n} = \frac{2}{M+2} \sum_{j=1}^{M+1} V_j^n H_1(t_{1j}), \ \ c_{2n} = \frac{2}{M+2} \sum_{j=1}^{M+1} V_j^n H_2(t_{2j}),
$$

in which $H_1(t_{1j})$ and $H_2(t_{2j})$ can be measured from Eq. (3.3) and Eq. (3.4), respectively. The SIF at the left point A_k and right point B_k can be assessed by

$$
(K_1 - iK_2)_{A_k} = (2\pi)^{1/2} \lim_{s \to s_{A_k}} \sqrt{|s - s_{A_k}|} \acute{\xi}_k(s),
$$

$$
(K_1 - iZ_2)_{B_k} = (2\pi)^{1/2} \lim_{s \to s_{B_k}} \sqrt{|s - s_{B_k}|} \acute{\xi}_k(s), \ \ k = 1, 2.
$$

where $\acute{\xi}_1(s)$ and $\acute{\xi}_2(s)$ are obtained from Eqs. (3.1) and (3.2), respectively [10].

5. Numerical results

In order to make the suggested method is comparable, numerical examples are presented. As mentioned earlier once, the two cracks being far apart the formulation in Eqs. (2.13) and (2.14) reduce to the equation for a single crack (Eq. (2.10)). For the straight crack with length $2a$, we obtain $K_1 = 1.0$ and $K_2 = 0.0$. Consider, two straight cracks in series, handled by the remote stress $\delta_y^\infty = \lambda$ (Fig.2(a) with $\alpha = 0$). The evaluated stress intensity factors at the cracks tips A, B, C, D are presented by

$$
\begin{aligned}
K_{1A} &= F_{1A}\left(\frac{a}{b}\right)\lambda(\pi a)^{\frac{1}{2}} \ , \ \ K_{2A} = F_{2A}\left(\frac{a}{b}\right)\lambda(\pi a)^{\frac{1}{2}}, \\
K_{1B} &= F_{1B}\left(\frac{a}{b}\right)\lambda(\pi a)^{\frac{1}{2}} \ , \ \ K_{2B} = F_{2B}\left(\frac{a}{b}\right)\lambda(\pi a)^{\frac{1}{2}}, \\
K_{1C} &= F_{1C}\left(\frac{a}{b}\right)\lambda(\pi a)^{\frac{1}{2}} \ , \ \ K_{2C} = F_{2C}\left(\frac{a}{b}\right)\lambda(\pi a)^{\frac{1}{2}}, \\
K_{1D} &= F_{1D}\left(\frac{a}{b}\right)\lambda(\pi a)^{\frac{1}{2}} \ , \ \ K_{2D} = F_{2D}\left(\frac{a}{b}\right)\lambda(\pi a)^{\frac{1}{2}}.
\end{aligned}
\tag{5.1}
$$

The calculated results are listed in Table 1, which display that our results are comparable with the previous works.

The SIFs at the crack points of $A, B, C,$ and D in terms of angle, α, are written as

$$
\begin{aligned}
K_{1A} &= F_{1A}(\alpha)\lambda\sqrt{\pi a} \ , \ \ K_{2A} = F_{2A}(\alpha)\lambda\sqrt{\pi a}, \\
K_{1B} &= F_{1B}(\alpha)\lambda\sqrt{\pi a} \ , \ \ K_{2B} = F_{2B}(\alpha)\lambda\sqrt{\pi a}, \\
K_{1C} &= F_{1C}(\alpha)\lambda\sqrt{\pi a} \ , \ \ K_{2C} = F_{2C}(\alpha)\lambda\sqrt{\pi a}, \\
K_{1D} &= F_{1D}(\alpha)\lambda\sqrt{\pi a} \ , \ \ K_{2D} = F_{2D}(\alpha)\lambda\sqrt{\pi a}.
\end{aligned}
\tag{5.2}
$$
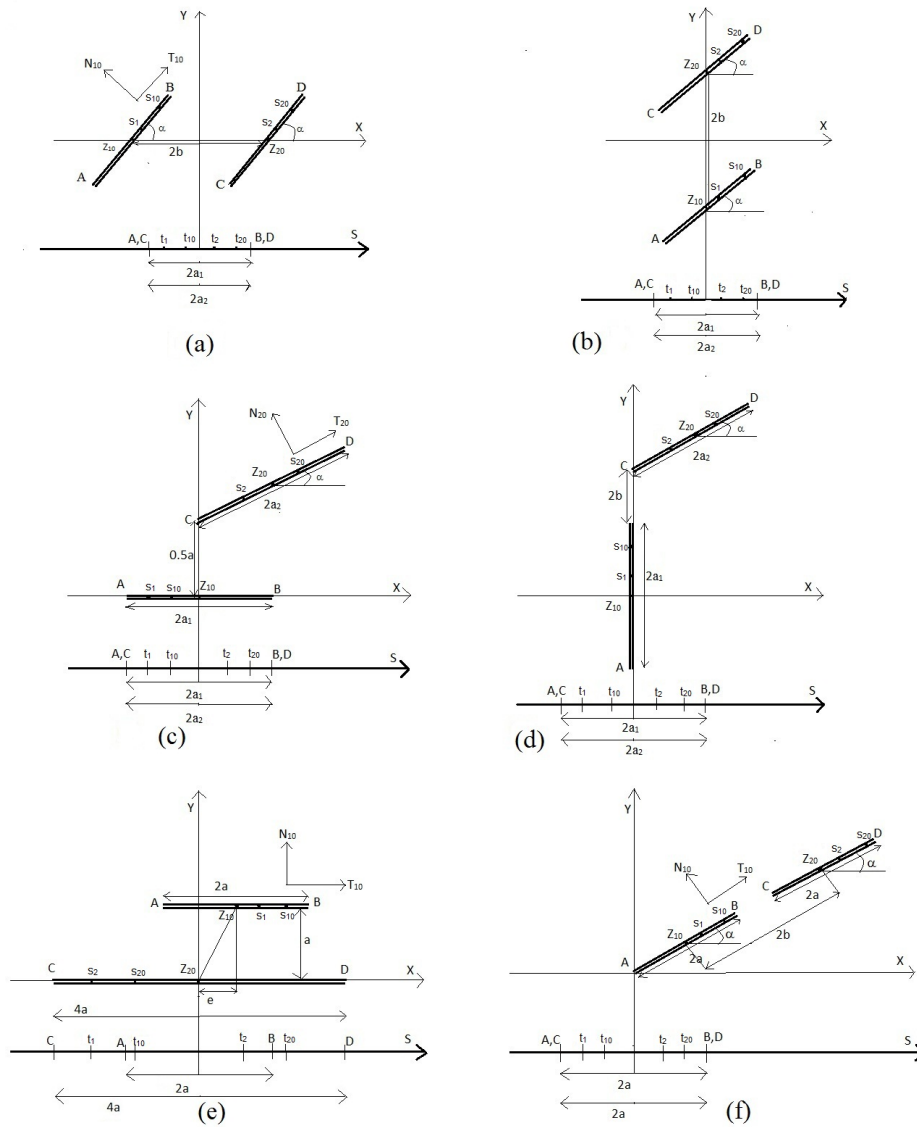
FIGURE 2. (a) Two series inclined cracks, (b) Two parallel inclined cracks, (c) A horizontal and an inclined cracks, (d) A prependicular and an inclined cracks, (e) Two straight cracks with different size, (f) Two inclined cracks in line. In cases a, b, c, d, we have $a_1 = a_2 = a$.

For another comparison example, the crack problem shown by Fig.5 is solved with two conditions $a/b = 0.9$ and $M = 15$. The computed results which are listed in

TABLE 1. The nondimensional SIF for two cracks in series.

a/b	0.1	0.2	0.3	0.4	0.5	0.6	0.7	0.8	0.9
F_{1A}									
m=15	1.00120	1.00462	1.01017	1.01787	1.02796	1.04094	1.05786	1.08017	1.11741
*m=15	1.00120	1.00462	1.01017	1.01787	1.02796	1.04094	1.05786	1.08017	1.11741
m=17	1.00120	1.00462	1.01017	1.01787	1.02796	1.04094	1.05786	1.08017	1.11741
*m=17	1.00120	1.00462	1.01017	1.01787	1.02796	1.04094	1.05786	1.08017	1.11741
F_{1B}									
m=15	1.00132	1.00566	1.01383	1.02717	1.04796	1.08040	1.13326	1.22894	1.45383
*m=15	1.00132	1.00566	1.01383	1.02717	1.04796	1.08040	1.13326	1.22894	1.45383
m=17	1.00132	1.00566	1.01383	1.02717	1.04796	1.08040	1.13326	1.22894	1.45387
*m=17	1.00132	1.00566	1.01383	1.02717	1.04796	1.08040	1.13326	1.22894	1.45387

*Chen[2]
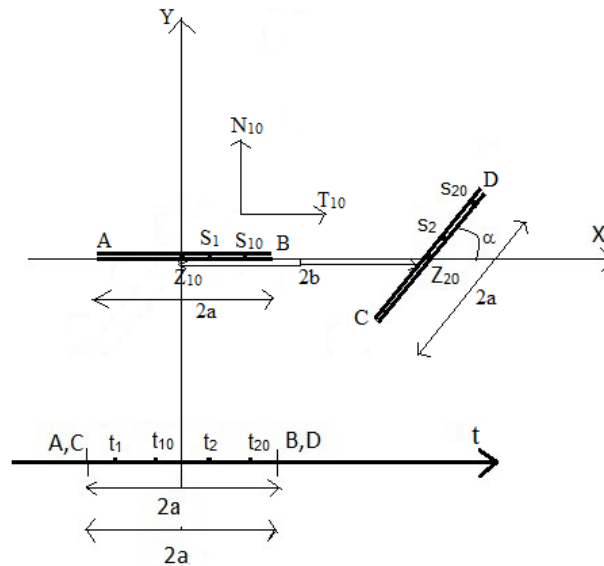
FIGURE 3. Two dissimilar cracks which the first crack is in horizontal position ($\alpha = 0$) with center on origin and the second in an inclined position with angle α.

Table 2 coincide with results were obtained by Chen(see [2]). Fig.4 shows that the nondimensional SIF for two inclined crack (Fig.2(a),(b)) is plotted against the angle α with $a/b = 0.9$. It is found that F_1's, for all crack tips, decrease with the increment of α (Fig.4(a)). The same behavior is found for parallel cracks (Fig.4(b)). For the serial cracks, the SIFs at B and C are slightly higher than SIFs at A and D (Fig.4(a)). F_2's at the crack points A, B, C, and D in two serial and parallel cracks (Fig.2(a,b)) are approximately the same because the cracks tend to either major or minor load axis. Fig.5 shows the influence of the distance that is located between two parallel cracks (Fig.2(b)). When the two cracks are closed together ($b/a < 0.1$), there is a fluctuate value of SIF (Fig.5(a)), and as b/a increases the SIF is almost constant (Fig.5(b)).

TABLE 2. The nondimensional SIF for two cracks which one crack
in horizontal position and another crack in an inclined position.

α	0	10	20	30	40	50	60	70	80	90
F_{1A}	1.1174	1.1197	1.1120	1.093	1.0719	1.0501	10301	1.0164	1.0071	1.0040
$*F_{1A}$	1.1174			1.0939			1.0300			1.0040
F_{1B}	1.4513	1.4859	1.4041	1.2938	1.2018	1.1299	1.0757	1.0375	1.0147	1.0071
$*F_{1B}$	1.4539			1.2931			1.0753			1.0071
F_{1C}	1.4513	1.4896	1.3007	1.0238	0.7556	0.5143	0.3105	0.1559	0.0604	0.0303
$*F_{1C}$	1.4539			1.0260			0.3133			0.0305
F_{1D}	1.1171	1.0925	1.0032	0.8567	0.6768	0.4867	0.3087	0.1630	0.0664	0.0303
$*F_{1D}$	1.1174			0.8568			0.3064			0.0305
F_{2A}	0	-0.0337	-0.0458	-0.0472	-0.0439	-0.0379	-0.0300	-0.0208	-0.0106	0
$*F_{2A}$	0			-0.0544			-0.0116			0
F_{2B}	0	-0.1369	-0.0939	-0.0663	-0.0548	-0.0475	-0.0394	-0.0285	-0.0150	0
$*F_{2B}$	0			-0.0522			-0.0035			0
F_{2C}	0	0.1074	0.3918	0.5589	0.6201	0.6006	0.5150	0.3771	0.2034	0.0132
$*F_{2C}$	0			0.5501			0.5118			0.0133
F_{2D}	0	0.1649	0.3254	0.4481	0.5136	0.5147	0.4523	0.3338	0.1727	-0.0132
$*F_{2D}$	0			0.4508			0.4526			-0.0133

*Chen[2]
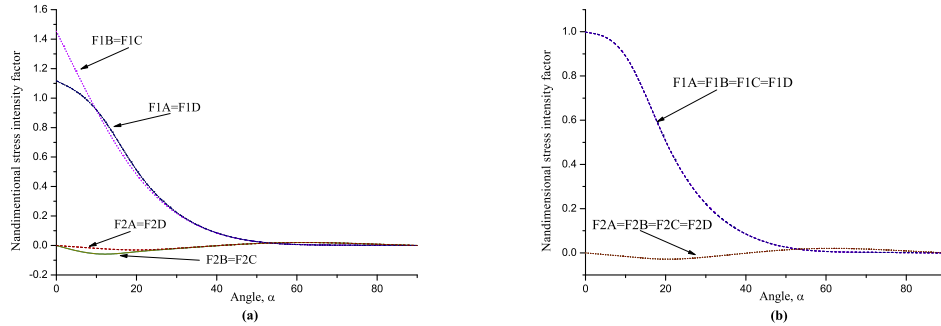
FIGURE 4. The nondimensional stress intensity factor for (a) Two
serial inclined cracks (Figure 2(a)), (b) Two parallel inclined cracks
(Figure 2(b)).

Fig.6(a) represents the interaction between two dissimilar, horizontal and inclined
cracks (Fig.2(c)). As α increases, F_{1A} slightly decreases whereas F_{1B} increases sig-
nificantly; then both of them tend to constant value. For the inclined crack, the SIF
decreases until it reaches its constant value. Fig.6(b) shows the interaction between a
perpendicular and an inclined cracks (Fig.2(d)). The SIFs decrease as α increases for
an inclined crack whereas for a perpendicular crack, the SIF is almost vanished. In
Fig.7, the effect of distance between a perpendicular and inclined crack is presented
(Fig.2(d)). If the two cracks are closed together ($b/a < 0.1$), then the magnitude
of SIFs at the tips of perpendicular crack decreases from 2 to almost 0 (Fig.7(a)),
whereas for $b/a > 0.1$ the SIFs are almost vanished (Fig.7(b)). Consider Fig.2(e).
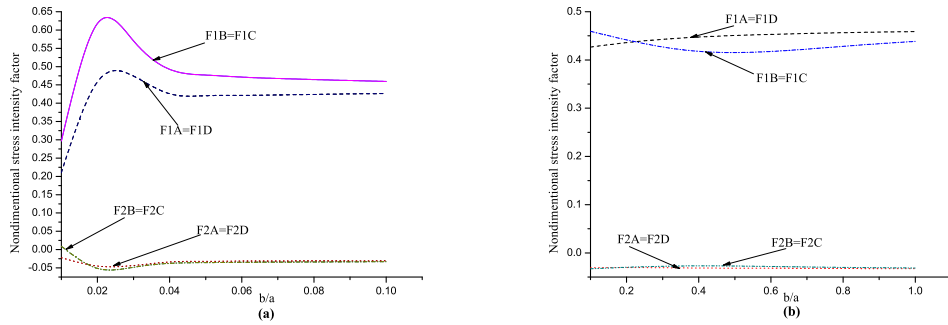
FIGURE 5. The nondimensional SIF for two parallel cracks with (a) $b/a < 0.1$ and (b) $b/a > 0.1$.
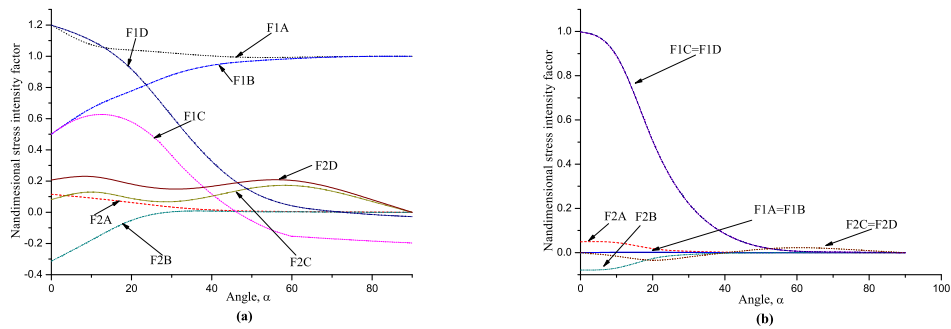
FIGURE 6. The nondimensional SIFs for (a) Horizontal and inclined cracks, (b) Perpendicular and inclined cracks.

The SIF at the crack tips is represented by

$$K_{1A} = F_{1A}\left(\frac{e}{a}\right)\lambda(\pi a)^{\frac{1}{2}}, \ \ K_{2A} = F_{2A}\left(\frac{e}{a}\right)\lambda(\pi a)^{\frac{1}{2}},$$
$$K_{1B} = F_{1B}\left(\frac{e}{a}\right)\lambda(\pi a)^{\frac{1}{2}}, \ \ K_{2B} = F_{2B}\left(\frac{e}{a}\right)\lambda(\pi a)^{\frac{1}{2}},$$
$$K_{1C} = F_{1C}\left(\frac{e}{a}\right)\lambda(\pi a)^{\frac{1}{2}}, \ \ K_{2C} = F_{2C}\left(\frac{e}{a}\right)\lambda(\pi a)^{\frac{1}{2}},$$
$$K_{1D} = F_{1D}\left(\frac{e}{a}\right)\lambda(\pi a)^{\frac{1}{2}}, \ \ K_{2D} = F_{2D}\left(\frac{e}{a}\right)\lambda(\pi a)^{\frac{1}{2}}. \tag{5.3}$$

The computed values are plotted in Fig.8(a). Fig.8(b) shows the interaction between two inclined crack for Fig.2(f).
The last example is allocated to two inclined crack that are located as series but they have different size (Fig.9). The calculated SIFs at the crack tips are stated by
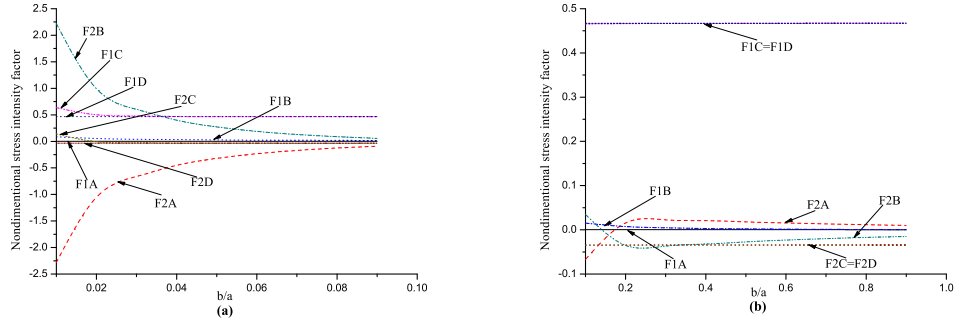
FIGURE 7.   The nondimensional SIFs for perpendicular and inclined cracks with (a) $b/a < 0.1$ and (b) $b/a > 0.1$.
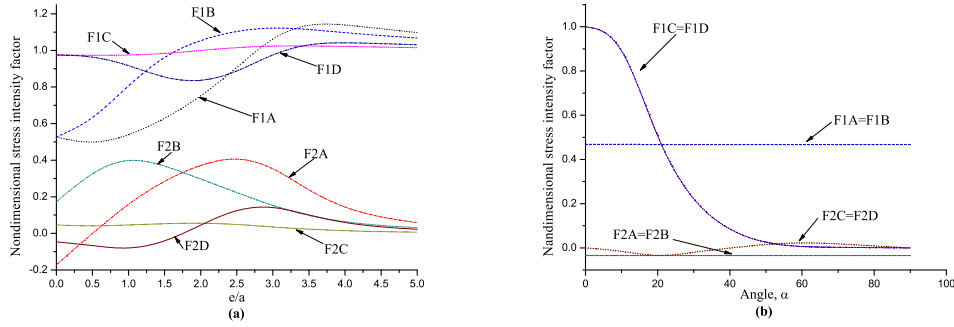
FIGURE 8.   The nondimensional SIFs (a) Two parallel cracks with different size (Figure 2(e)), (b) Two inclined cracks (Figure 2(f)).

$$K_{1A} = F_{1A}\left(\frac{b}{a_1}\right)\lambda\sqrt{\pi a} \ , \ \ K_{2A} = F_{2A}\left(\frac{b}{a_1}\right)\lambda\sqrt{\pi a},$$

$$K_{1B} = F_{1B}\left(\frac{b}{a_1}\right)\lambda\sqrt{\pi a} \ , \ \ K_{2B} = F_{2B}\left(\frac{b}{a_1}\right)\lambda\sqrt{\pi a},$$

$$K_{1C} = F_{1C}\left(\frac{b}{a_1}\right)\lambda\sqrt{\pi a} \ , \ \ K_{2C} = F_{2C}\left(\frac{b}{a_1}\right)\lambda\sqrt{\pi a},$$

$$K_{1D} = F_{1D}\left(\frac{b}{a_1}\right)\lambda\sqrt{\pi a} \ , \ \ K_{2D} = F_{2D}\left(\frac{b}{a_1}\right)\lambda\sqrt{\pi a}. \tag{5.4}$$

Fig.10(a) represents that the nondimentional SIFs for two inclined crack with different size decrease when the angle increases and F_2 at all crack tips are approximately the same because the cracks tend to load axis (major or minor). The effect of the distance between two cracks with different size is shown in Fig .10(b). As we can see that,
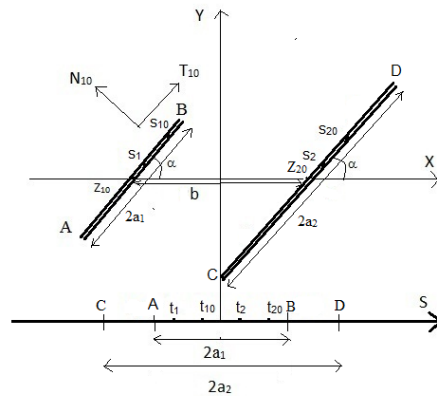
FIGURE 9. Two inclined crack that are located as series with different size.
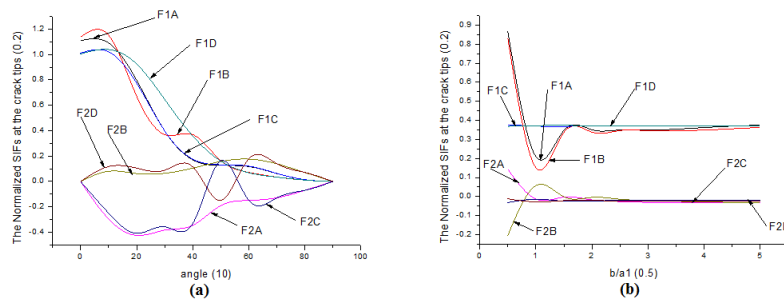
FIGURE 10. The nondimensional SIFs (a) Two inclined crack with different size when the angle is variable, (b) Two inclined crack with different size when the distance between them is variable.

when two cracks are closed together, the SIFs are high; whereas when they are getting farther apart, the SIFs reach to constant value, meanwhile F_2 in all crack tips is almost vanished.

6. CONCLUSION

The multiple cracks problems in an infinite plate is formulated into hieq based on complex potential method. With the aid of the appropriate quadrature formulas, the obtained hieq is solved numerically for function that is unknown. The stress intensity factor at the crack tips is evaluated. It is found that once the cracks are closed together the SIF is increased and as those are getting far the SIF is almost constant at crack tips. Our results for the serial cracks is agree with the previous work of Chen (see [2]).

References

[1] Y. Z. Chen and Y. K. Cheung, *New integral equation approach for plane crack problem in elastic half-plane.* International Journal Fracture, *46* (1990), 57–69.

[2] Y. Z. Chen, *Hypersingular integral equation approach for the multiple crack problem in an infinite plate.*Acta Mechanica, *108* (1995), 121–131.

[3] Y. Z. Chen, *Numerical solution of multiple crack problem by using hypersingular integral equation.*International Journal of Fracture, *88* (1997), L9– L14.

[4] Y. Z. Chen, *Numerical solution of a curved crack problem by using hypersingular integral equation approch.*Engineering Fracture Mechanics, *46* (1993), 275–283.

[5] Y. Z. Chen, *New singular integral equation for curve crack problem in plane elastisity.*International Journal Fracture, *49* (1990), 39–43.

[6] Y. Z. Chen, *A numerical solution technique of hypersingular integral equation for curved cracks.*Communication in Numerical Method in Engineering, *19* (2003), 645–655.

[7] Y. Z. Chen and X. Y. Lin,*Complex potentials and integral equations for curved crack and curved rigid line problems in plane elasticity.*Acta Mechanica, *182* (2006), 211–229.

[8] Y. K. Cheung and Y. Z. Chen, *New integral equation for plane elasticity crack problem.*Theoretical Applied Fracture Mechanic, *7* (1987), 177–184.

[9] B. Cotterell and J. R. Rice, *Slitghtly curved or kinked cracks.*International Journal of Fracture, *16* (1980), 155–169.

[10] Y. Z. Chen, *A procedure for regularization of singular integral equation of the multiple crack problem in an infinite plate.*International Journal of Fracture, *34* (1987), R53–R56.

[11] M. Erfanian and H. Zeidabadi, *Using of Bernstein spectral Galerkin method for solving of weakly singular VolterraFredholm integral equations*, Mathematical Sciences, Springer. *12* (2018), 103–109.

[12] F. Erodogan, *Stress intensity factors.*Journal of Applied Mechanic, *50* (1983), 992–1002.

[13] J. Hadamard, *Lectures on Cauchy's problem in linear differential equations.*Yale, University Press, Noordhoff, Leyden, 1st edition, 1923.

[14] N. I. Ioakimidis, *Mangler type principal value integral in hypersingular integral equation for crack problem in plane elasticity.*Engineering of Fracture Mechanic, *31* (1988), 895–898.

[15] A. C. Kaya and F. Erodogan, *On the solution of integral equation with strongly singular kernels.*Quarterly of Applied Mathematics, *45* (1987), 105–122.

[16] N. I. Muskhelishvili, *Some basic problem of the mathematical theory of elasticity.* Noordhoff, The Netherlands, Noordhoff, The Netherlands, 1st edition, 1953.

[17] K. Mayrhofer and F. D. Fischer, *Derivation of a new analytical solution for a general two dimensional finite–part integral applicable in fracture mechanics.* International Journal of Numerical Method in Engineering, *33* (1992), 1027–1047.

[18] H. F. Nied, *Periodic arrary of cracks in half-plane subjected to arbitrary loading.*Journal of Applied Mechanic, *54* (1987), 642–648.

[19] N. M. A. Nik Long and Z. K. Eshkuvatov, *Hypersingular integral equation for multiple curved cracks problem in plane elasticity*, International Journal of Solids and Structures, *46* (2009), 2611–2617.

[20] V. Z. Parton and P. I. Perlin, *Integral equation in elasticity*, Mir, Moscow, Mir, Moscow, 1st edition, 1982.

[21] M. P. Savruk, *Two-dimentional problems of elasticity for body with crack*, kiev, Naukava, Dumka, kiev, Naukava, Dumka, 1st edition, 1981.

[22] G. C. Sih, *Methods of analysis and solution of crack problem*, Mechanic of Fracture, Noordhoff, Leyden, 1st edition, 1973.

[23] S.S irajo Lawan Bichi, K. Eshkuvatov and N. M. A. NikLong, *An Automatic Quadrature Schemes and ErrorEstimates for Semibounded Weighted Hadamard TypeHypersingular Integrals*, Abstract and Applied Analysis, (2014), Article ID 387246, 13 pages.

[24] W. L. Zang and P. Gudmundson, *Kinked cracks in an anisotropic plane modeled by an integral equation method*, International Journal Solids Structure, *14* (1991), 1855–1865.